

X-ray activity cycle on the active ultra-fast rotator AB Dor A? Implication of correlated coronal and photometric variability

S. Lalitha and J. H. M. M. Schmitt

Hamburger Sternwarte, University of Hamburg, Gojenbergsweg 112, 21029 Hamburg, Germany
e-mail: lalitha.sairam@hs.uni-hamburg.de

Received XXXX; accepted XXXX

ABSTRACT

Context. Although chromospheric activity cycles have been studied in a larger number of late-type stars for quite some time, very little is known about coronal activity-cycles in other stars and their similarities or dissimilarities with the solar activity cycle.

Aims. While it is usually assumed that cyclic activity is present only in stars of low to moderate activity, we investigate whether the ultra-fast rotator AB Dor, a K dwarf exhibiting signs of substantial magnetic activity in essentially all wavelength bands, exhibits an X-ray activity cycle in analogy to its photospheric activity cycle of about 17 years and possible correlations between these bands.

Methods. We analysed the combined optical photometric data of AB Dor A, which span ~35 years. Additionally, we used ROSAT and XMM-Newton X-ray observations of AB Dor A to study the long-term evolution of magnetic activity in this active K dwarf over nearly three decades and searched for X-ray activity cycles and related photometric brightness changes.

Results. AB Dor A exhibits photometric brightness variations ranging between $6.75 < V_{mag} \leq 7.15$ while the X-ray luminosities range between $29.8 < \log L_X [erg/s] \leq 30.2$ in the 0.3-2.5 keV. As a very active star, AB Dor A shows frequent X-ray flaring, but, in the long XMM-Newton observations a kind of basal state is attained very often. This basal state probably varies with the photospheric activity-cycle of AB Dor A which has a period of ~17 years, but, the X-ray variability amounts at most to a factor of ~2, which is, much lower than the typical cycle amplitudes found on the Sun.

Key words. stars: activity – stars: coronae – stars: late-type – stars: individual: AB Dor

1. Introduction

One of the key characteristics of the Sun is its 11-year activity cycle, which was originally discovered from the periodic variation in the observed sunspot numbers (Schwabe 1844). However, the solar cycle also manifests itself in many other activity indicators such as the solar 10.7 cm radio emission, its chromospheric Ca II emission, and its coronal X-ray emission (Gnevyshev 1967; Hathaway 2010). Ever since Hale (1908) discovered strong magnetic fields in sunspots, the magnetic character of solar activity and its cyclic variations has been beyond dispute. The cycle variations in the solar corona are far more pronounced than those observed in the photosphere, and with the advent of space-based astronomy vast amounts of solar X-ray data have been collected, which allow a better understanding of the evolution of coronal plasma temperature, emission measure, and structure over the solar cycle (Orlando et al. 2000). As expected, the solar corona has a distinctly different appearance during activity minimum than encountered at activity maximum. The solar X-ray flux varies during a cycle by typically a factor of ~ 200 in the energy range of 0.6-1.5 keV (Kreplin 1970), while Stern et al. (2003) computed the solar soft X-ray irradiance variations as measured by the *Yohkoh* satellite in the 0.5-4 keV energy range and found a maximum- to minimum- ratio of ~ 30. Tobiska (1994) estimated a variation of a factor of ~10 in the softer energy range between 0.25-0.4 keV as the solar activity cycle progresses. The cause for these substantial flux variations is the absence of large active regions in the solar corona during its activity minimum, which make it appear much fainter than the solar corona during

the activity maximum (Golub 1980). However, the amplitude of these variations sensitively depends on the energy range considered and becomes much smaller at softer energies. For example, Ayres (1997) and Ayres et al. (2008) argued that through the 0.1-2.4 keV ROSAT pass band, the Sun was expected to show variations between the minimum and maximum flux of a factor of 5-10. Peres et al. (2000) estimated the X-ray brightness of the Sun during activity maximum and minimum to be $\log L_X = 27.5$ erg/s and $\log L_X = 26.5$ erg/s, respectively, in the ROSAT 0.1-2.4 keV energy band, which would mean a variation of order of magnitude variation in the ROSAT band. Their results were supported by the studies of Orlando et al. (2000) and Judge et al. (2003), who also estimated variations of about a factor of ~10 in the solar coronal X-ray emission throughout the solar cycle.

The question then immediately arises whether other late-type stars also show such a solar-like cyclic variability in their magnetic activity properties (Vaughan et al. 1978; Wilson 1978). Within the context of the Mt. Wilson HK program the long-term variability of stellar chromospheric activity (as observed in the Ca II emission cores) in a large sample of late-type stars was systematically studied over several decades and the cyclic activity of a larger number of stars in the solar neighbourhood was established (Baliunas et al. 1995). Specifically, Baliunas et al. (1998) found that about 60% of the stars of the Mt. Wilson observatory survey exhibited periodic and cyclic variations, and furthermore, Lockwood et al. (2004, 2007) found evidence that the photospheric and chromospheric activity cycle are related. Baliunas et al. (1995) employed the same technique of studying stellar activity to also monitor the solar activity-cycle in integrated light and showed that the so-called S-index of the Sun

Send offprint requests to: S. Lalitha

varies between 0.16 and 0.22 between its activity minima and maxima; in fact, the Sun shows one of the most regular cycles in the whole stellar sample presented by Baliunas et al. (1998).

A related question is whether the stars with different cyclic properties in their Ca II emission show a different behaviour with respect to their coronal emission. Hempelmann et al. (1996) compared soft X-ray fluxes with Ca emission in a sample of late-type stars and showed that the stars with cyclic variations in their calcium flux tend to show less X-ray activity than stars with irregular variability in their Ca II emission. Additionally, X-ray faint stars tend to show flat activity curves or low levels of short-term variability (see Wright et al. 2010 and references therein). On the other hand, X-ray bright, active stars are believed to have no long-term cycles; instead, they are thought to exhibit an irregular variation in their X-ray luminosity (Stern 1998). Currently, only fewer than handful of stars have been found to have long-term X-ray cycles (cf. Fig. 8). With ROSAT, the monitoring of the visual binary 61 Cyg began that subsequently was continued with *XMM-Newton* (Hempelmann et al. 2006). Four more stars, which are the α Cen system, HD 81809, and τ Boo, were also monitored by *XMM-Newton* (Favata et al. 2004, 2008; Robrade et al. 2007; Ayres 2009; Robrade et al. 2012; Poppenhaeger et al. 2012) for possible cyclic variations. Favata et al. (2004) detected a pronounced cycle of 8.2 years and a clear evidence for large-amplitude X-ray variability in phase with the chromospheric activity cycle for HD 81089. For 61 Cyg A, Robrade et al. (2012) found a regular coronal activity cycle in phase with its 7.3 yr chromospheric cycle, whereas no evidence of a clear coronal cycle for 61 Cyg B could be produced. Furthermore, these authors demonstrated that the two α Cen stars exhibit significant long-term X-ray variability, with α Cen A showing a cyclic variability over a period of 12-15 years, while the α Cen B data suggest an X-ray cycle of a period of 8-9 years; the amplitudes of the variability for α Cen A and B were estimated to be an order of magnitude and about a factor six to eight, respectively. In addition, Robrade and collaborators also concluded that the coronal activity cycles are a common phenomenon in older, slowly rotating G and K stars. It is worthwhile noting that most of these stars were moderately or low active. However, recently Sanz-Forcada et al. (2013) showed an X-ray cycle of ~ 1.6 years in the active planet-hosting star ι Hor, demonstrating that short cycles in Ca II also have an X-ray equivalent. On the other hand, Poppenhaeger et al. (2012) studied the activity cycle associated with τ Boo, a moderately active F-star displaying a magnetic cycle of ~ 1 year, as anticipated from Zeeman Doppler imaging, but they were unable to find any evidence of an activity cycle with the available X-ray data.

We study the behaviour of coronal X-ray emission during the activity cycle and a possible correlation between the photospheric and X-ray activity in the very active star AB Dor A. Our paper is structured as follows: in Sect. 2 we present the target stars and in Sect. 3 we describe the observations and data analysis. In Sect. 4 we discuss the optical and X-ray light curves and also discuss our investigation on the correlation between the photospheric and coronal activity cycles. In Sect. 5, we compare our target with other stars that show cyclic behaviour. In Sect. 6 we investigate the short-term variation induced by the star's rotation, and we close with a summary in Sect. 7.

2. Our target star

AB Dor is a quadruple system consisting of the components AB Dor A, AB Dor Ba, AB Dor Bb, and AB Dor C. AB Dor A

is a magnetically active young dwarf-star of spectral type K0, located at a distance of ~ 15 pc from the Sun as a foreground star of the Large Magellanic Cloud (LMC). It is a very rapid rotator with a period of $P = 0.514$ days and $v \sin i \approx 90$ Km/s (see Guirado et al. 2011 and references therein), resulting in very high levels of magnetic activity with an average $\log(L_x/L_{bol}) \approx -3$. Located $9.5''$ away from AB Dor A is an active M dwarf AB Dor B (Rst 137B; Vilhu & Linsky 1987; Vilhu et al. 1989), about ~ 60 times bolometrically fainter than AB Dor A, and therefore only little or no contamination due to the presence of AB Dor B is expected in data that leave both components unresolved. At radio wavelengths AB Dor B was serendipitously detected with the Australian Telescope Compact Array (ATCA) during an observations of AB Dor A (Lim et al. 1992). However, the binarity of AB Dor B itself with a separation of only $0.7''$ (called AB Dor Ba and AB Dor Bb) was detected only after the advent of adaptive optics. Yet another low-mass companion to AB Dor A is AB Dor C Guirado et al. (1997), located about $0.16''$ away from AB Dor A.

The apparent magnitude of AB Dor A of $V=6.75$ (Amado et al. 2001) makes it a favourite target for optical observations with the aim of monitor photospheric spots and performing Doppler imaging (Rucinski 1983; Innis et al. 1986, 1988; Kuerster et al. 1994; Anders 1994; Unruh et al. 1995). Additionally, Järvinen et al. (2005) noted evidence for a possible activity cycle of ~ 20 years along with a flip-flop cycle of ~ 5.5 years. Innis et al. (2008) repeated the cycle study with new data and determined a cycle period supporting the ~ 20 year period suggested by Järvinen et al. (2005).

AB Dor A has not only been a target of interest for optical observations, but has been observed with many space-based observatories across the UV, EUV, and X-ray wavebands. The first X-ray detection of AB Dor A was obtained with the *Einstein* Observatory (Pakull 1981; Vilhu & Linsky 1987), and ever since then AB Dor A has been observed repeatedly by almost all X-ray observatories (Collier Cameron et al. 1988; Vilhu et al. 1993; Mewe et al. 1996; Maggio et al. 2000; Güdel et al. 2001; Sanz-Forcada et al. 2003a; Hussain et al. 2007; Lalitha et al. 2013). The long-term X-ray behaviour of the X-ray emission from the AB Dor system is dominated by AB Dor A (Güdel et al. 2001; Sanz-Forcada et al. 2003a). AB Dor Ba and Bb cannot be separated with current X-ray telescopes; the combined luminosity of the B-components is $\sim 2.8 \times 10^{28}$ erg/s in the 0.2-4.0 keV (Vilhu & Linsky 1987). Sanz-Forcada et al. (2003a) obtained a luminosity of $\sim 3.4 \times 10^{28}$ erg/s in the 0.5-2.0 keV with *Chandra* ACIS observations. Hence, the contribution of the companions to the X-ray emission of AB Dor A can be considered negligible, essentially because the quiescent X-ray emission of the companions scales as their bolometric luminosity.

The time evolution of AB Dor A has previously been studied by Kuerster et al. (1997), who compared the V-band brightness with X-ray observations (5 1/2 years of observations) carried out by the ROSAT satellite, but they found no pronounced long-term activity period from their analysis because the 5 1/2 years of data available at the time barely cover a part of the activity cycle. The same applies to the studies of Sanz-Forcada et al. (2007), who noted a weak increasing trend in the X-ray emission using the observations carried out by *XMM-Newton* that cover about six years of observations.

3. Observations and data analysis

3.1. X-ray data

Because it is a foreground star of the LMC, AB Dor has the advantage of being easily observable at all times with most X-ray satellites, and therefore quite a number of often serendipitously taken X-ray data of this source exist. We used *ROSAT* observations¹ listed in the *ROSAT* Position Sensitive Proportional Counters (PSPC) source catalogue from pointed observations with typical exposure times of between 1 ksec and 3 ksec, and the *ROSAT* High Resolution Imager (HRI) source catalogue again from pointed observations with typical exposure times of between 1 ksec and 6 ksec. Since the *ROSAT* satellite was in a low Earth orbit, the typical contiguous and uninterrupted viewing intervals of a source are typically in the range 1 - 2 ksec, therefore longer exposures are composed of a number of shorter exposures with sometimes very long intervening temporal gaps. We specifically used the PSPC observations obtained between 1990 and 1993 and the HRI observations obtained between 1990 and 1998; the total PSPC exposure is 74.4 ksec, the total HRI exposure is 106.2 ksec; thus, the *ROSAT* observations comprise a relatively short total exposure time when compared with the *XMM-Newton* observations listed in Table 1.

We also carried out a detailed analysis of AB Dor A, using the data obtained by *XMM-Newton* Observatory. On board *XMM-Newton* three telescope are co-aligned with three CCD cameras (i.e., one PN and two MOS cameras) with a sensitivity range between ≈ 0.2 and 15 keV, which together form the European Photon Imaging Camera (EPIC). The X-ray telescopes equipped with MOS detectors are also equipped with reflection gratings. These two reflection-grating spectrometers (RGS) provide high spectral resolution ($E/\Delta E \approx 200-800$) in the energy range 0.35-2.5 keV. Useful data were obtained from the EPIC and the RGS detectors (see Tab. 1 for a detailed account).

AB Dor A, which is a very bright target with many emission lines, is fortuitously used as a calibration source for the *XMM-Newton* RGS. Hence this target has been repeatedly observed over the last decade, giving us an ideal opportunity to assess the long-term behaviour of AB Dor A. In these data there are either no observations or typically much shorter observation time covered by the EPIC instrument than that of the RGS (see Tab. 1); we therefore restricted our analysis to the available RGS data. The data were reduced using the standard *XMM-Newton* Science Analysis System (SAS) software V12.0.1. We used the meta-task *rgsproc* 1.30.3 to process the RGS data, followed by the spectral extraction and response generation. To create a combined light curve of the two instruments (RGS1+RGS2) the task *rgslccor* 0.52.1 was used².

In Fig. 1, we provide all RGS light curves³ used for our analysis, and indicate the times of quiescence and strong flaring. Because AB Dor A is an active star, flaring is indeed observed in almost all observations. When investigating the long-term behaviour of AB Dor A, we focused on the quiescent emission. Hence we excluded time periods of enhanced activity or strong flaring, particularly when the count rate increased from the quiescent level by about 50 or more percent for each observation. We thus excluded larger flares on the basis of the respective X-ray light curve and calculated the mean or median count rate for

the combined RGS (RGS1+RGS2) observations (see Col. 4 in Tab. 1).

Table 1. Observation log of *XMM-Newton* data. Columns 4 and 5 provide the mean RGS/median RGS count rate and the data dispersion for the RGS data.

Obs. ID	Date	Obs. time PN/RGS [ks]	Mean/median RGS count rate [cts/s]	σ of the RGS data points [cts/s]
2000				
0123720201	01/05	60.0/49.9	2.64/2.62	0.32
0126130201	07/06	41.9/58.9	2.58/2.57	0.29
0123720301	27/10	55.7/58.8	2.82/2.80	0.26
0133120701	11/12	6.2/8.8	3.07/3.00	0.18
0133120101	"	13.4/60.4	3.15/3.13	0.21
0133120201	"	4.2/20.8	3.03/3.03	0.21
2001				
0134520301	20/01	48.6/52.2	3.81/3.80	0.21
0134520701	22/05	48.2/49.5	2.58/2.57	0.38
0134521301	13/10	— /39.6	2.76/2.74	0.26
2002				
0134521501	12/04	15.9/53.1	3.63/3.66	0.28
0155150101	18/06	4.9/20.3	3.74/3.68	0.36
0134521601	"	21.3/47.8	3.80/3.77	0.350
0134521801	05/11	— /19.8	3.86/3.80	0.11
0134521701	15/11	— /19.8	2.50/2.50	0.32
0134522001	03/12	— /22.3	3.93/3.91	0.28
0134522101	30/12	— /48.8	3.31/3.31	0.30
2003				
0134522201	23/01	— /51.8	2.17/2.19	0.17
0134522301	30/03	— /48.8	3.64/3.59	0.38
0134522401	31/05	— /28.8	2.95/2.97	0.22
0160362701	23/10	— /26.5	2.79/2.80	0.23
0160362801	08/12	— /53.7	3.67/3.63	0.30
2004				
0160362901	27/11	— /56.3	2.60/2.59	0.28
2005				
0160363001	18/04	— /52.1	2.57/2.58	0.38
0160363201	16/10	— /50.1	2.54/2.51	0.25
2006				
0412580101	31/12	— /44.9	2.96/2.87	0.40
2007				
0412580201	19/07	— /48.8	3.32/3.35	0.42
2008				
0412580301	03/01	— /48.8	2.78/2.77	0.27
2009				
0412580401	04/01	47.0/48.8	2.56/2.53	0.32
0602240201	25/11	57.9/58.3	2.15/2.12	0.23
2010				
0412580601	11/01	9.9/49.8	2.21/2.20	0.24
2011				
0412580701	02/01	9.9/62.8	2.51/2.522	0.21
0412580801	31/12	9.9/61.8	2.68/2.67	0.22

¹ The *ROSAT* observation log is provided in electronic form at CDS.

² A detailed description of the *XMM* packages is available at <http://xmm.esac.esa.int/sas/current/doc/packages.All.html>

³ After revolution 135, the CCD 7 in RGS1 suffered a failure; this failure does affect comparisons between observations using count rates.

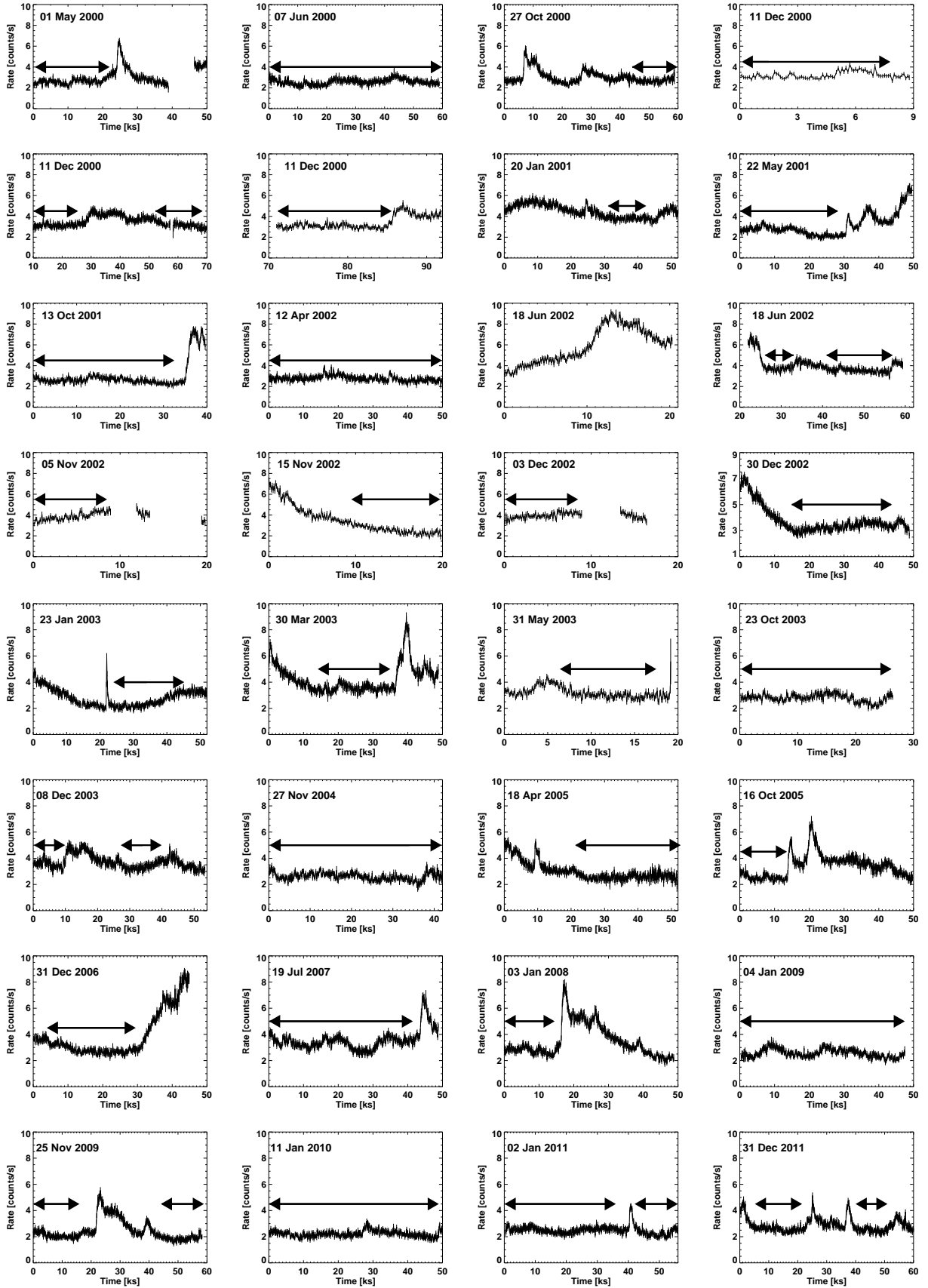


Fig. 1. XMM-RGS light curves of AB Dor A plotted in counts per second. Quiescent time intervals are marked by arrows; see text for details. A log of the observations is provided in Table 1.

3.2. Optical data

We compiled all publicly available photometric V-band data of AB Dor A, covering nearly 34 years of observations taken between 1978-2012 with a short gap between 1998-1999 and 2000-2001. The data taken between 1978-2000 have been presented by Järvinen et al. (2005); most of the observations were carried out using the standard Johnson *UBVRI* filters. Additionally, we used an – unpublished – data set collected between 2001-2012 obtained in the context of the all-sky automated survey (ASAS)⁴ in the V band (Pojmanski 1997; Pojmanski et al. 2005), which is publicly available.

ASAS is a CCD photometric sky survey, monitoring the southern as well as a part of the northern sky ($\delta < +28^\circ$) since 2000 up to now. The ASAS telescope is located in Chile, Las Campanas Observatory (LCO), at an altitude of 2215 m above sea level and consists of two wide field ($9^\circ \times 9^\circ$) cameras equipped with both V and I filters. For AB Dor A, we used observations carried out using only V-band data with exposure times of 180s for each frame; in general, the photometric accuracy of ASAS data for AB Dor A is about 0.05 mag.

4. Long term light curves

4.1. Optical light curves

In Figure 2, we plot the V-band brightness of AB Dor A as a function of time. We then subdivided the entire ~ 34 years of V-band observations into smaller time periods and estimated a median V magnitude over each of these time bins (depicted as black and blue circles).

To search for periodic variability we performed a periodogram analysis on the entire optical dataset using the generalised Lomb-Scargle periodogram in the form introduced by Zechmeister & Kürster (2009), which is a variant of the Lomb-Scargle periodogram. In Figure 3, we show the resulting periodogram from the entire optical data set spanning nearly 34 years of observations. A clear peak around ≈ 6190 days (corresponding to 16.96 years) is apparent, which is highly significant, given the derived false-alarm probabilities (FAP), also shown in Fig. 3. As a next step we fitted a sine wave with a period of ~ 16.96 years to the the entire data set presented in Fig. 2 after correcting for the linear trend in the Järvinen et al. (2005) and the ASAS data set (plotted as orange curve in Fig. 2). Additionally, in Fig. 4 we plot the mean of optical data folded with the cycle period of ≈ 17 years.

In addition to the main peak in Fig. 3, we note another peak with a period of ≈ 1 year that has a $FAP \approx 10\%$. To determine whether this period is due to the activity cycle we recomputed the periodogram after subtracting the best-fit sine wave with $P = 16.96$ years from the observed data. When comparing both the periodograms it became evident that the high peak with a period of ≈ 1 year persists, hence this peak cannot be the result of considerable spectral leakage from the cycle frequency. Therefore, the nature of this peak remains unclear, but we assume that it is caused by the seasonal distribution of the observations.

4.2. X-ray light curves

Lockwood et al. (1997) and Radick et al. (1998) studied the relationship between the photometric variability and chromospheric activity of Sun-like stars by combining the Mount Wilson HK

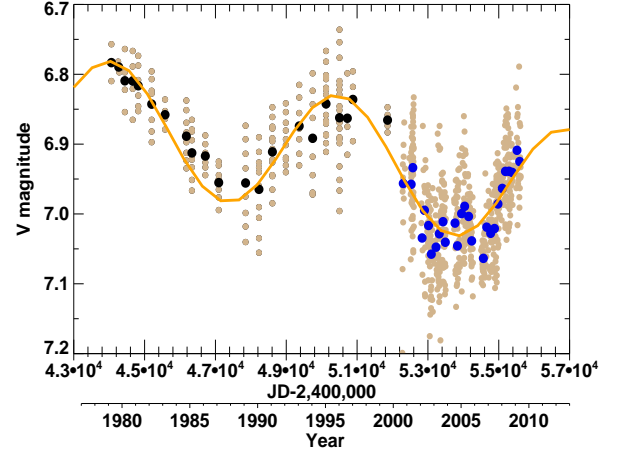


Fig. 2. AB Dor A long-term V-band brightness evolution adapted from Järvinen et al. (2005) and ASAS observations. The brown circles denote all individual V-band observations. The estimated median magnitudes are denoted as black and blue circles for the data from Järvinen et al. (2005) and the ASAS observations, respectively. Plotted as a thick line is the sinusoidal fit to the entire dataset with a period of ≈ 17 years.

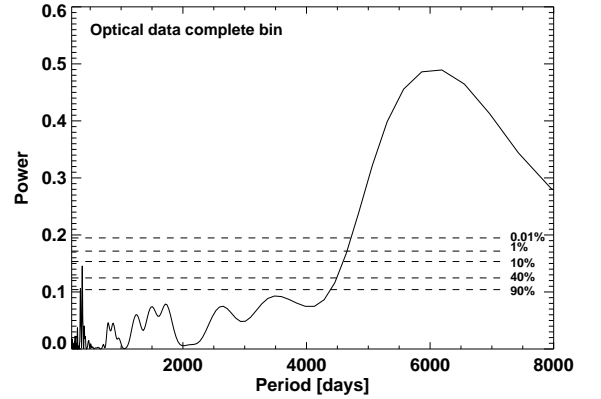


Fig. 3. Periodogram of complete data set of optical V-mag brightness. The highest peak indicates activity-cycle period values of 16.96 years.

activity observations with 11 years of Strömgren *b* and *y* photometry taken at Lowell Observatory. The latter authors found that on cycle time-scales young active stars show an inverse correlation between photometric brightness and chromospheric activity, while older stars such as the Sun show a direct correlation between brightness and activity. Radick et al. (1998) explained this finding by arguing that the stars switch from spot-dominated to facular-dominated brightness variations at an age of ≈ 2 Gyr. If the same pattern of variation applies to AB Dor A, one would expect spot-dominated brightness variation, since AB Dor A is a very young star with an age of ~ 50 Myr (Close et al. 2005). Hence, according to Fig. 2, one would expect an increase in X-ray activity from minimum to maximum between 1996-2004, and a decline in X-ray activity between 1990-1996 and also since 2005. In this section we therefore investigate to what extent the available X-ray data support the view of such cyclic coronal activity in AB Dor A.

⁴ The ASAS data are available at <http://www.astrouw.edu.pl/asas/>

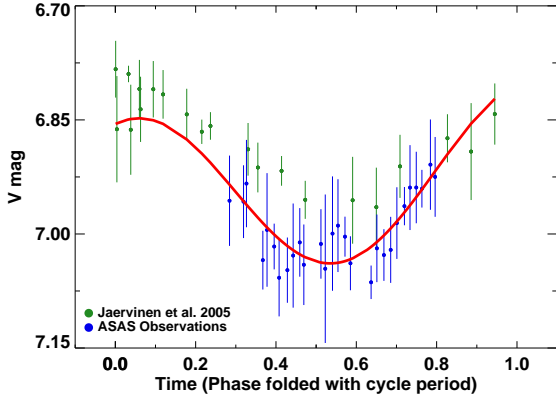


Fig. 4. Optical V-band brightness data of Fig. 2 folded with a cycle period of 16.96 years versus the phase interval [0.0,1.0]. Plotted in green and blue are the mean of the Järvinen et al. (2005) and ASAS observations, respectively; the plotted error bar depicts the brightness measurement distribution due to rotational modulation.

4.2.1. Overall X-ray behaviour

In Figure 5, we show the temporal behaviour of the soft X-ray luminosity as observed between 1990 and 2011 by various X-ray satellites. Assuming that AB Dor-A’s X-ray spectrum can be described with temperature components 2 and 5 MK and an equivalent absorption column N_H of 10^{18} cm^{-3} , we computed energy conversion factors (ECF) to convert the observed count rates into fluxes. Using XSPEC v12.6.0 and WebPIMMS v4.6, we estimated $ECF_{PSPC} = 6.42 \times 10^{-12} \text{ erg/cm}^2/\text{counts}$, $ECF_{HRI} = 3.03 \times 10^{-11} \text{ erg/cm}^2/\text{counts}$, $ECF_{RGS1} = 4.44 \times 10^{-11} \text{ erg/cm}^2/\text{counts}$, and $ECF_{RGS2} = 5.68 \times 10^{-11} \text{ erg/cm}^2/\text{counts}$ in the canonical ROSAT energy band 0.1–2.4 keV; the resulting X-ray luminosities (L_X) were finally calculated using a distance of $14.9 \pm 0.1 \text{ pc}$ (Guirado et al. 2011).

We performed a periodogram analysis on the X-ray light curve presented in Fig. 5, but we were unable to obtain a significant peak indicating any preferred period. Subsequently, we used the period obtained from the optical light curve assuming that the optical period also applies to the X-ray data. We folded the X-ray light curve with this period and obtained a sinusoidal fit to the X-ray data (depicted as a black thick line). While this sinusoidal curve provides a description of the data, it is far from unique and there is very large scatter around the fit curve, casting some doubt on signatures of cyclic activity in the X-ray range.

4.2.2. Correlation between X-ray and optical data

To examine whether the trends in the X-ray and optical are really correlated, we carried out a correlation analysis of the two data sets. To relate an optical magnitude to each X-ray observation, we used the value of the fitted optical light curve (see Fig. 2) at the time of each X-ray observation. The resulting scatter plot is shown in Fig. 6, where we show logarithmic X-ray luminosity vs. V-band magnitude. A linear fit between those quantities gives a slope of 0.9 ± 0.2 for the correlation of $\log L_X$ with V_{mag} , implying that the X-ray luminosity is higher when the photospheric brightness is lower. Furthermore, we also computed a linear Pearson correlation coefficient (ρ) of 0.40 between the X-ray luminosity and photospheric brightness with a two-tailed

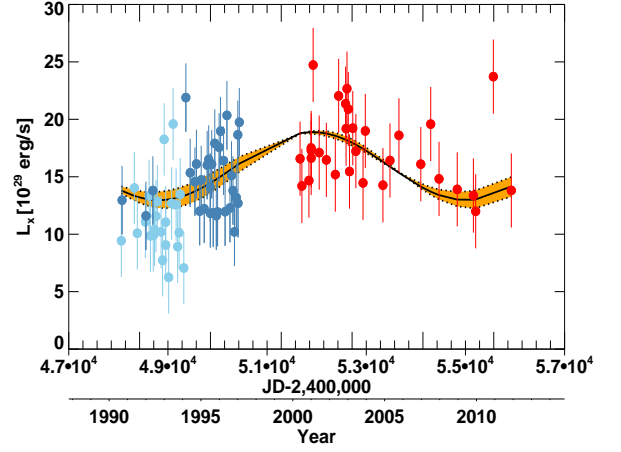


Fig. 5. Temporal behaviour of the soft X-ray luminosity with 1σ deviation as observed by several X-ray missions between 1990 and 2011. ROSAT PSPC data are plotted as light-blue filled circles; ROSAT HRI data are depicted as navy-blue filled circles. The red circles represent XMM-Newton RGS observations. Plotted as a thick black curve is sinusoidal fit to the X-ray data with an optical-cycle period of ≈ 17 years.

probability value of 0.0001%. These findings are clearly consistent with the picture that the star is X-ray bright when the surface brightness is low.

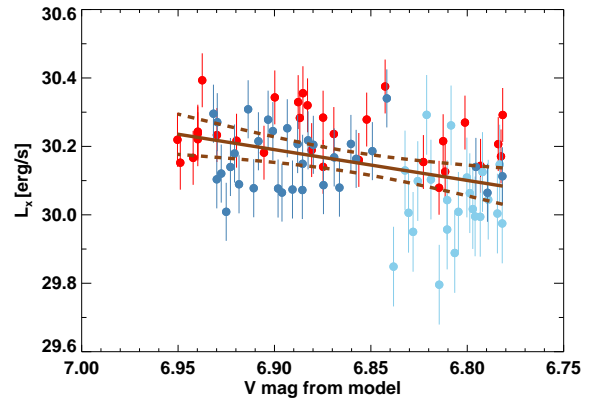


Fig. 6. Variation of X-ray luminosity as a function of the (calculated) V magnitude. The symbols here are the same as in Fig. 5; see text for details. Plotted as brown lines are the linear regression with 2σ confidence band.

4.2.3. Individual light curves: ROSAT

While the overall X-ray light curve might be affected by errors in the instrumental cross calibrations, trends in individual instruments should be free from such effects and be real. In the following we therefore concentrated on the data taken with the ROSAT PSPC and the ROSAT HRI, from which a multitude of observations is available, to determine count-rate trends individually for each instrument. We found a negative slope with respect to the time evolution of the count rates for the ROSAT PSPC data,

Table 2. Results from the search for a long-term variation in the X-ray data. The errors and the false-alarm probability (FAP) are obtained from bootstrapping the observed distribution of the measurements (BS).

Data set	best fit slope [cts/sec/yr]	Error BS	FAP %
<i>ROSAT</i>			
PSPC	-0.22	0.47	72
HRI	0.05	0.05	61
<i>XMM</i> RGS	-0.04	0.02	63

while for the ROSAT HRI data we found a faint positive slope (see column 2 in Table 2).

We used a simple bootstrap technique to estimate the error of the slope. For this purpose we ran a Monte Carlo simulation for the observing times, carrying out linear fits to the simulated data sets. The count rates and their individual errors were randomly redistributed over the range of available observing times. A regression analysis on the re-sampled data was performed and repeated several times (5×10^5 times), thus providing an error at 1σ probability associated with the determined slope. The results of this analysis are listed in column 3 of Table 2. For the PSPC data we found that in 72% of the cases slopes as small as the observed one are obtained by pure chance, whereas for the HRI data this is estimated to be true in 61% of the cases.

Comparing the optical light curve (Fig. 2) and the X-ray light curve (Fig. 5), one expects the ROSAT PSPC observations to be at activity minimum during the 17-year cycle, the ROSAT HRI observations to be during the constant or rise phase from minimum to maximum activity level and the *XMM-Newton* observations cover almost half an activity-cycle period. Our regression analysis of the individual PSPC and HRI data is consistent with this picture, but the statistical significance is low.

4.2.4. Individual light curves: *XMM-Newton*

Since AB Dor A was used as a calibration source for *XMM-Newton*, many datasets with much enhanced quality and long temporal coverage of AB Dor A have become available, which can be used for cycle studies. In contrast to the ROSAT observations, those of *XMM-Newton* are much longer, which allows us to identify periods of flaring in the data stream and exclude these periods from analysis. In Fig. 7 we plot the evolution of the XMM-RGS count rate taking into consideration only the quiescent emission. In addition, we re-plot Fig. 2 to compare the optical and X-ray light curves (the lower panel of Fig. 7). If the XMM-RGS data show a variation similar to the optical data, 2000-2006 should represent the activity maximum. Because visual inspection suggests an anti-correlation between the optical and the X-ray data, we carried out some statistical tests to determine whether these trends are significant or not.

A (parametric) regression analysis on these data similar to the ROSAT data was performed, and the results are presented in Table 2 as well. We obtained a negative slope for the observed XMM-RGS count rates as a function of time, and again, similar to the ROSAT data, we performed a simple bootstrap technique to estimate the error of the slope and FAP. A slope as small as the observed one for the XMM-RGS data that occurs by pure chance is estimated to be 63%. The negative slope fits with the overall picture of an expected decline in the activity, but the significance of this slope is again very low.

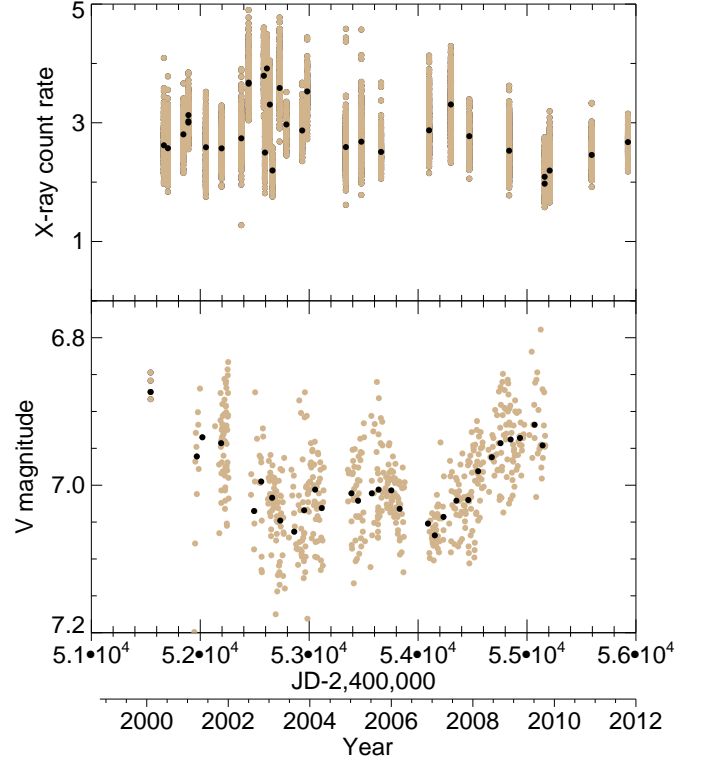


Fig. 7. Top panel: Temporal behaviour of the XMM-RGS count rate binned to 100 s (as brown circles) after removing the flares from each observation. The median count rate over the duration of each observational run is depicted as black circles. Bottom panel: V-band data for AB Dor A (same as Fig. 2).

We then decided to apply non-parametric correlation tests such as the Spearman ρ and Kendall τ test (Press 1992) on the mean and the median XMM-RGS data presented in Table 1. For this purpose we divided the XMM-RGS data into two subsets, one covering the years 2000-2005, that is, towards the anticipated maximum, and the second set between 2005-2011 with declining activity. The Spearman rank correlation coefficient ρ is defined as

$$\rho = \frac{\sum(R_i - \bar{R})(S_i - \bar{S})}{\sqrt{\sum(R_i - \bar{R})^2} \sqrt{\sum(S_i - \bar{S})^2}}, \quad (1)$$

where R_i and S_i are the ranks of time and the minimum count-rate values respectively. The significance of a non-zero value of ρ is computed from a parameter t defined as

$$t = \rho \sqrt{\frac{N-2}{1-\rho^2}}, \quad (2)$$

where ρ is the Spearman rank and N is the sample size. Note that the significance t is distributed approximately as a Student distribution with $N-2$ degrees of freedom (Press 1992); a low value of significance (p in Tab. 3) indicates a significant correlation.

An alternative non-parametric test is the Kendall τ -test, which uses the relative ordering of the rank instead of the numerical difference of the ranks. Consider two samples (with n items each) of physical quantities, in our case the observing times t_i ($i = 1, N$) and the minimum count rate r_i ($i = 1, N$); we assumed

Table 3. Results from the correlation test performed on the mean and median XMM-RGS data. Column 3 shows the significance of a non-zero value of the Spearman rank, and Column 5 shows whether the observed value of τ is significantly different from zero.

Data set	Spearman ρ test			Kendall τ test	
	ρ	t	p-value	τ	σ^2
Mean RGS data					
2000-2005	-0.01	-0.07	0.94	0.02	0.02
2005-2011	-0.45	-1.33	0.22	-0.28	0.07
2000-2011	-0.36	-2.15	0.04	-0.22	0.01
Median RGS data					
2000-2005	-0.05	-0.22	0.82	0.01	0.02
2005-2011	-0.33	-0.94	0.37	-0.22	0.07
2000-2011	-0.35	-2.05	0.04	-0.20	0.01

the times to be sorted so that $t_i < t_{i+1}$. The total number of possible pairs of time and count rates is $n(n-1)/2$. We considered a pair of values of time t and count rate r . If the relative ordering of the ranks of two observing times is the same as the relative ordering of the two rates, the pair is called concordant, otherwise the pair is called discordant. Ignoring the problem of how to treat timed observations, the basic idea is to compare the number of concordant and discordant pairs, since that number should be statistically equal in the absence of correlations. Specifically, the Kendall τ is given by

$$\tau = \frac{n_c - n_d}{n(n-1)/2}, \quad (3)$$

where n_c is the number of concordant and n_d the number of discordant pairs, normalised by the total number of pairs. Clearly, for a perfect correlation $\tau = 1$. On the null hypothesis of independence of time and count rate, that is, no correlation, τ is expected to be normally distributed with zero expectation and a variance of

$$Var(\tau) = \frac{4N + 10}{9N(N-1)}. \quad (4)$$

The results of our correlation analysis are provided in Tab. 3, where we also quote the two-sided probability value (p-value) for a given t-value (Eqn. 2). Clearly, the two tests on the median and mean RGS data yield no significant correlations for the 2000 - 2005 data, while they suggest significant correlations for both the median and mean RGS data between 2000 - 2011. If only the 2005 - 2011 data are considered, the τ -test suggests a significant correlation, while the correlation is marginal at best using the Spearman rank ρ . In **all** cases, however, there is an anti-correlation, that is, the X-ray rate is decreasing according to expectation. These results suggest that there is an influence of the activity cycle on the X-ray emission, but the observed X-ray variation is quite different from the X-ray variation measured for the Sun. It is of course difficult to assess this influence quantitatively, but inspecting the values provided in Tab. 1, we find a maximum count-rate of 3.93/3.91 cts/s from XMM-RGS data and a minimum count-rate of 2.15/2.12 cts/s, from which we calculate a variation amplitude of at most ~ 1.8 in the X-ray emission between lowest and highest activity in AB Dor A, which is consistent with previous findings reported by Sanz-Forcada et al. (2003b).

4.3. Summary: Is there an X-ray activity cycle on AB Dor A ?

While a clear cyclic behaviour with a cycle length of ~ 17 years is observed for AB Dor A in its optical brightness variations, a similar variation in the available X-ray data is not immediately apparent. However, Fig. 6 suggests an anti-correlation between optical and X-ray brightness in support of the view of a variation in X-ray flux with the optical cycle. The extensive and contiguous observations carried out with the XMM-Newton RGS allow a much more refined assessment of the temporal variability of AB Dor A than all previously available X-ray data. An inspection of Fig. 1 demonstrates that AB Dor A is variable at all times and does indeed produce frequent and significant flaring. However, the XMM-Newton RGS data also demonstrate that AB Dor A returns to a basal state at around approximately 3 RGS cts/sec. This basal state can be observed only in reasonably long and contiguous observations, and even then it may not be attained. At any rate, in short and non-contiguous data, as available from satellites in low Earth orbit such as ROSAT, it is difficult to identify such basal state periods; still, taking the ROSAT data at face value, the data support a variation of X-ray flux with optical cycle in the anticipated way, although the obtained correlations are not statistically significant.

Since the available XMM-Newton observations now cover the period between optical activity maximum and minimum, we carried out several statistical tests to study a possible activity cycle associated with the XMM-RGS data. The results indeed indicate an increase and decline in activity with an activity maximum around 2002-2003 (cf. Fig.7). This change in activity manifests itself in a change in the flux of the basal state level, but the change in amplitude is at most a factor of two, and possibly even lower. As a consequence, the relative change is far less than the relative change observed in the Sun and other late-type stars and therefore the variability of the star's basal state is weaker than the typical X-ray variability (outside flares) in less active cool stars. The low-amplitude variability observed in AB Dor A may be attributed to the fact that we are dealing with an ultra-fast rotator that has a saturated corona.

5. Comparison of AB Dor A's activity cycle with that of other stars

In the following section we view our findings on the activity cycle on AB Dor A in the context of stellar activity cycles as seen in X-rays and other activity indicators. In Fig. 8, we plot the cycle period (in years) vs. the stellar rotation period (in days) for the sample stars. We use the stellar sample discussed in detail by Brandenburg et al. (1998) and Böhm-Vitense (2007) (blue and green triangles), the stars with confirmed X-ray cycles discussed in the introduction section (magenta circles) and individual fast rotators with activity cycles as discussed by Bernhard & Frank (2006), Taš (2011), and Vida et al. (2013) (red circles); the data point for AB Dor A is also shown, using its 0.52-day rotation period and 17-year activity-cycle period.

Brandenburg et al. (1998) showed that active and inactive stars follow different branches in a P_{cyc} - P_{rot} -diagram. Böhm-Vitense (2007) suggested that the time taken for the toroidal magnetic field to reach the stellar surface is determined by the length of the activity cycle associated with the star. Hence studying the relation between the rotation period and the length of the activity cycle may shed light on the relevant dynamo mechanisms.

Most of the X-ray cycle stars fit the active or inactive sequence proposed by Brandenburg et al. (1998) and

Böhm-Vitense (2007) reasonably well. Note that the short-period systems follow yet different branches in the P_{cyc} - P_{rot} diagram. We hypothesise that AB Dor A and other ultra-fast rotators have somewhat different dynamo processes that are not readily comparable to more slowly rotating stars. Clearly, substantial work needs to be done to demonstrate the reality of *activity cycles* in ultra-fast rotators as a class.

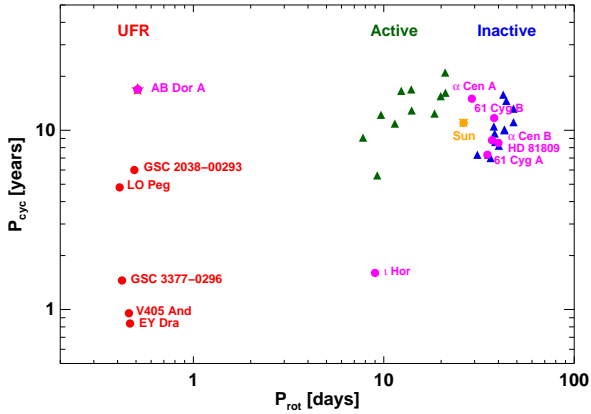


Fig. 8. Rotation period plotted as a function of the activity-cycle period. Depicted as blue and green triangles are stars belonging to inactive and active sequence (Böhm-Vitense 2007). Represented as a magenta circles are stars with X-ray cycles (cf. see introduction). The place of AB Dor A is represented as magenta star. Depicted as red circles are the activity cycles reported in other ultra-fast rotators reported by Bernhard & Frank (2006), Taš (2011), and Vida et al. (2013).

6. Rotational modulation

Out of the wealth of data of available *XMM-Newton* data on AB Dor A, we chose the subsets of data that cover more than one stellar rotation and are therefore well suited for a short-term variability study. In Fig. 9, we depict the X-ray light curve after flares were removed by eye for all *XMM-RGS* data sets with more than one rotational period and plot this vs the rotational phase interval. We note substantial fluctuations as a result of an active corona. The seemingly irregular variability seen in individual light curves can be attributed to the low energy and short time-scale flares, with no obvious sign of rotational modulation. We point out that the data shown in Fig. 9 extend over ten years, yet the dispersion of the data is very low, re-emphasizing the existence of a possible basal coronal state in AB Dor A.

7. Summary

The available X-ray observations of AB Dor A, compiled for a period of more than two decades, show X-ray variability on a variety of time scales. Since AB Dor A is a very active star, it exhibits substantial short-term variability and in particular frequent flaring activity. This flaring activity may last for several hours and can be observed in *XMM-Newton* data where the exposure time ranges over several tens of kilo-seconds (cf. Fig. 1). But in short and non-contiguous snapshot observations typically available from low Earth-orbit satellites such as the ROSAT observations, which typically have individual exposure times of a

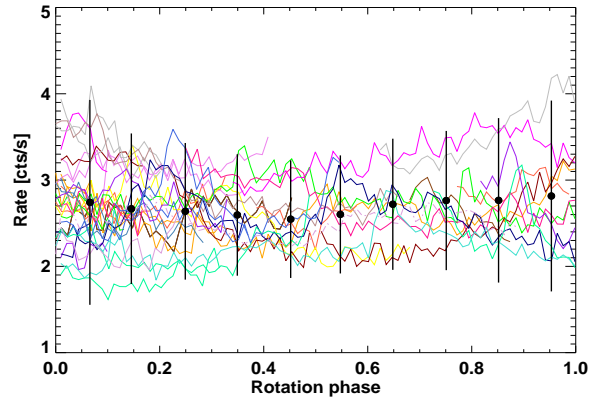


Fig. 9. X-ray light curve after removing the flares from a subset of *XMM-RGS* observation on AB Dor A folded with rotational period and plotted vs. the phase interval. Each colour represents different observations/ different rotation. Represented as black filled circles are mean count rate at a certain rotation phase with 2σ deviation.

few kilo-seconds at best, this variability is difficult to distinguish from variability on longer time-scales. In the optical, long-term variability with a period of 16-17 years that is highly reminiscent of the solar sunspot cycle could be established; with 20% the amplitude of the optical cyclic variations is quite substantial.

Because of its substantial variability on short time-scales, a correlation between X-ray and photospheric activity is difficult to establish with snapshot X-ray data. However, in sufficiently long X-ray observations of AB Dor A, we were able to estimate a basal state of ≈ 3 *XMM-Newton* RGS cts/sec. Furthermore, we presented evidence that this basal state flux may vary with the optical cycle of AB Dor A in analogy to the solar activity cycle; note that the Sun appears faintest when large Sun spot group(s) are on its visible hemisphere. However, for AB Dor A we estimated a factor of only ~ 1.8 variation in the X-ray emission in 0.3-2.5 keV range during its cycle, and therefore this very active star is in some sense much less variable than other solar-like stars (Rohrabe et al. 2012), albeit the basic picture that the X-ray flux is highest, when the photospheric brightness is at lowest, also seems to apply to AB Dor A.

Clearly, the time interval for which X-ray and optical data are available is very short compared to the assumed cycle period of almost 17 years. Only two cycles have been covered so far, and a true periodicity as observed for the Sun is far from established. Furthermore, photometric monitoring of AB Dor A and related objects in the next decades is certainly in order to study whether the observed variations are truly cyclic with a well-defined period. With more or less robotic facilities such monitoring can today be carried out at relatively low cost. Similarly, extended X-ray observations of AB Dor A and again similar objects would help in establishing the existence of such basal states in other stars, as well, and also their relationship to stellar parameters and possible cycle variations.

Acknowledgements. S. L. acknowledges funding by the DFG in the framework of RTG 1351 "Extrasolar planets and their host stars".

References

Amado, P. J., Cutispoto, G., Lanza, A. F., & Rodonò, M. 2001, in *Astronomical Society of the Pacific Conference Series*, Vol. 223, 11th Cambridge Workshop

- on Cool Stars, Stellar Systems and the Sun, ed. R. J. Garcia Lopez, R. Rebolo, & M. R. Zapaterio Osorio, 895–900
- Anders, G. J. 1994, *Information Bulletin on Variable Stars*, 3985, 1
- Ayres, T. R. 1997, *J. Geophys. Res.*, 102, 1641
- Ayres, T. R. 2009, *ApJ*, 696, 1931
- Ayres, T. R., Judge, P. G., Saar, S. H., & Schmitt, J. H. M. M. 2008, *ApJ*, 678, L121
- Baliunas, S. L., Donahue, R. A., Soon, W., & Henry, G. W. 1998, in *Astronomical Society of the Pacific Conference Series*, Vol. 154, *Cool Stars, Stellar Systems, and the Sun*, ed. R. A. Donahue & J. A. Bookbinder, 153
- Baliunas, S. L., Donahue, R. A., Soon, W. H., et al. 1995, *ApJ*, 438, 269
- Bernhard, K. & Frank, P. 2006, *Information Bulletin on Variable Stars*, 5719, 1
- Böhm-Vitense, E. 2007, *ApJ*, 657, 486
- Brandenburg, A., Saar, S. H., & Turpin, C. R. 1998, *ApJ*, 498, L51
- Close, L. M., Lenzen, R., Guirado, J. C., et al. 2005, *Nature*, 433, 286
- Collier Cameron, A., Bedford, D. K., Rucinski, S. M., Vilhu, O., & White, N. E. 1988, *MNRAS*, 231, 131
- Favata, F., Micela, G., Baliunas, S. L., et al. 2004, *A&A*, 418, L13
- Favata, F., Micela, G., Orlando, S., et al. 2008, *A&A*, 490, 1121
- Gnevyshev, M. N. 1967, *Sol. Phys.*, 1, 107
- Golub, L. 1980, *Royal Society of London Philosophical Transactions Series A*, 297, 595
- Güdel, M., Audard, M., Briggs, K., et al. 2001, *A&A*, 365, L336
- Guirado, J. C., Marcaide, J. M., Martí-Vidal, I., et al. 2011, *A&A*, 533, A106
- Guirado, J. C., Reynolds, J. E., Lestrade, J.-F., et al. 1997, *ApJ*, 490, 835
- Hale, G. E. 1908, *ApJ*, 28, 315
- Hathaway, D. H. 2010, *Living Reviews in Solar Physics*, 7, 1
- Hempelmann, A., Robrade, J., Schmitt, J. H. M. M., et al. 2006, *A&A*, 460, 261
- Hempelmann, A., Schmitt, J. H. M. M., & Stępień, K. 1996, *A&A*, 305, 284
- Hussain, G. A. J., Jardine, M., Donati, J.-F., et al. 2007, *MNRAS*, 377, 1488
- Innis, J. L., Budding, E., Olah, K., et al. 2008, *Information Bulletin on Variable Stars*, 5832, 1
- Innis, J. L., Thompson, K., & Coates, D. W. 1986, *MNRAS*, 223, 183
- Innis, J. L., Thompson, K., Coates, D. W., & Evans, T. L. 1988, *MNRAS*, 235, 1411
- Järvinen, S. P., Berdyugina, S. V., Tuominen, I., Cutispoto, G., & Bos, M. 2005, *A&A*, 432, 657
- Judge, P. G., Solomon, S. C., & Ayres, T. R. 2003, *ApJ*, 593, 534
- Kreplin, R. W. 1970, *Annales de Geophysique*, 26, 567
- Kuerster, M., Schmitt, J. H. M. M., & Cutispoto, G. 1994, *A&A*, 289, 899
- Kuerster, M., Schmitt, J. H. M. M., Cutispoto, G., & Dennerl, K. 1997, *A&A*, 320, 831
- Lalitha, S., Fuhrmeister, B., Wolter, U., et al. 2013, *A&A*, submitted
- Lim, J., Nelson, G. J., Castro, C., Kilkenny, D., & van Wyk, F. 1992, *ApJ*, 388, L27
- Lockwood, G. W., Radick, R. R., Henry, G. W., & Baliunas, S. L. 2004, in *Bulletin of the American Astronomical Society*, Vol. 36, *American Astronomical Society Meeting Abstracts #204*, 671
- Lockwood, G. W., Skiff, B. A., Henry, G. W., et al. 2007, *ApJS*, 171, 260
- Lockwood, G. W., Skiff, B. A., & Radick, R. R. 1997, *ApJ*, 485, 789
- Maggio, A., Pallavicini, R., Reale, F., & Tagliaferri, G. 2000, *A&A*, 356, 627
- Mewe, R., Kaastra, J. S., White, S. M., & Pallavicini, R. 1996, *A&A*, 315, 170
- Orlando, S., Peres, G., & Reale, F. 2000, *ApJ*, 528, 524
- Pakull, M. W. 1981, *A&A*, 104, 33
- Peres, G., Orlando, S., Reale, F., Rosner, R., & Hudson, H. 2000, *ApJ*, 528, 537
- Pojmanski, G. 1997, *Acta Astron.*, 47, 467
- Pojmanski, G., Pilecki, B., & Szczygiel, D. 2005, *Acta Astron.*, 55, 275
- Poppenhaefer, K., Günther, H. M., & Schmitt, J. H. M. M. 2012, *Astronomische Nachrichten*, 333, 26
- Press, W. 1992, *Numerical recipes in C : the art of scientific computing* (Cambridge Cambridge New York: Cambridge University Press)
- Radick, R. R., Lockwood, G. W., Skiff, B. A., & Baliunas, S. L. 1998, *ApJS*, 118, 239
- Robrade, J., Schmitt, J. H. M. M., & Favata, F. 2012, *A&A*, 543, A84
- Robrade, J., Schmitt, J. H. M. M., & Hempelmann, A. 2007, *Mem. Soc. Astron. Italiana*, 78, 311
- Rucinski, S. M. 1983, *A&AS*, 52, 281
- Sanz-Forcada, J., Maggio, A., & Micela, G. 2003a, *A&A*, 408, 1087
- Sanz-Forcada, J., Maggio, A., & Micela, G. 2003b, *A&A*, 408, 1087
- Sanz-Forcada, J., Micela, G., & Maggio, A. 2007, in *XMM-Newton: The Next Decade*, 3P
- Sanz-Forcada, J., Stelzer, B., & Metcalfe, T. S. 2013, *A&A*, 553, L6
- Schwabe, M. 1844, *Astronomische Nachrichten*, 21, 233
- Stern, R. A. 1998, in *Astronomical Society of the Pacific Conference Series*, Vol. 154, *Cool Stars, Stellar Systems, and the Sun*, ed. R. A. Donahue & J. A. Bookbinder, 223
- Stern, R. A., Alexander, D., & Acton, L. W. 2003, in *The Future of Cool-Star Astrophysics: 12th Cambridge Workshop on Cool Stars, Stellar Systems, and the Sun*, ed. A. Brown, G. M. Harper, & T. R. Ayres, Vol. 12, 906–911
- Taš, G. 2011, *Astronomische Nachrichten*, 332, 57
- Tobiska, W. K. 1994, *Sol. Phys.*, 152, 207
- Unruh, Y. C., Collier Cameron, A., & Cutispoto, G. 1995, *MNRAS*, 277, 1145
- Vaughan, A. H., Preston, G. W., & Wilson, O. C. 1978, *PASP*, 90, 267
- Vida, K., Kriskovics, L., & Oláh, K. 2013, *ArXiv e-prints*
- Vilhu, O., Ambruster, C. W., Neff, J. E., et al. 1989, *A&A*, 222, 179
- Vilhu, O. & Linsky, J. L. 1987, *PASP*, 99, 1071
- Vilhu, O., Tsuru, T., Collier Cameron, A., et al. 1993, *A&A*, 278, 467
- Wilson, O. C. 1978, *ApJ*, 226, 379
- Wright, N. J., Drake, J. J., & Civano, F. 2010, *ApJ*, 725, 480
- Zechmeister, M. & Kürster, M. 2009, *A&A*, 496, 577